03.1

Impulse impact on the wall upon the interaction of a shock with an ellipsoidal near-wall gas bubble of increased density

© A.G. Sirenko, O.G. Sutyrin

Institute of Mechanics of Lomonosov Moscow State University, Moscow, Russia
E-mail: sutyrin@imec.msu.ru

Received April 27, 2023
Revised June 13, 2023
Accepted June 13, 2023

Based on the numerical solution of the Euler equations, the problem of the interaction of a shock wave with an ellipsoidal gas bubble of increased density adjacent to a solid wall is studied. The process of refraction and focusing of the shock wave is described - the formation and reflection of transverse shock waves from the axis of symmetry and from the wall. It is found that, depending on the shape of the bubble, qualitatively different flow regimes take place, in which the focusing of the wave on the axis of symmetry occurs before or after the beginning of the reflection of the wave transmitted through the bubble from the wall. The grid convergence of various measures of impulse shock impact on the wall is studied and their dependence on the bubble shape is determined. The highest pressure impulse is achieved for slightly flattened bubbles, when the transverse waves are focused near the center of the wall immediately after the plane transmitted wave is reflected from it.

Keywords: shock wave, gas bubble, wall, shock focusing, cumulation.

DOI: 10.61011/TPL.2023.08.56693.19608

The problem of interaction between a shock wave and gas bubbles of a different density or chemical composition (shock-bubble interaction) [1] is being studied internationally in the context of its applications in astrophysics and combustion of gaseous mixtures. In recent years, the concomitant effect of focusing, which may induce combustion and detonation in flammable gaseous mixtures [2], has attracted increased interest. Two major types of focusing (external and internal) are distinguished [3]; the intensity of focusing depends to a considerable extent both on the intensity of an incident wave and on the parameters of a bubble: on the gas density and, in particular, on the bubble shape.

The evolution of vortices and jets in flows with sequential impact of an incident shock wave and a shock wave reflected off the dead end of a shock tube on a gas bubble is being examined fairly extensively [4,5]. However, the influence of a gas bubble on the impulse shock impact on a wall remains understudied, although this issue is of interest in the context of explosive safety and as a basis for construction of novel types of devices (gas-dynamic punchers and injectors). The attenuation of this impact on a solid sphere with a light gas bubble present in front of it has been investigated in [6]. The case of a near-wall bubble of an increased density has been examined for the first time in [7] in the plane formulation. It has been demonstrated that the peak pressure on a wall increases many-fold in the presence of a bubble due to the effect of shock wave focusing and depends to a considerable extent on the density of gas in a bubble and on its positioning.

In the present study, the interaction of a shock wave with near-wall bubbles of spherical and ellipsoidal shapes is examined in the axially symmetric formulation, and the impulse impact on a wall is estimated based on integral measures.

A plane shock wave propagates from left to right within a uniform ideal gas at rest that contains an ellipsoidal bubble of gas of an increased density adjacent to a solid impenetrable wall positioned transverse to the wave propagation direction (Fig. 1). The pressure and density of gas in front of a shock wave were taken as unity, and the parameters of gas behind the wave were specified by the Rankine–Hugoniot conditions. The defining parameters of the problem are Mach number M of the incident wave, density of gas ω in a bubble, ratio of semi-axes $\chi = l/w$ of the bubble, and adiabatic exponent γ of gas. Air ($\gamma = 1.4$) is both the background gas and the gas in the bubble. The bubble diameter at $\chi = 1.0$ was taken as a unit of length. The slip condition was set at the right boundary of the calculation domain (solid wall), and simplified „nonreflecting“ conditions $\frac{\partial}{\partial n} = 0$ were set at the other boundaries. In contrast to our previous study [7], we examine only the case of immediate adjacency of the bubble to the wall. A mode of bubble–wall contact („quarter-diameter cutoff“) providing, under otherwise equal conditions, the greatest impulse impact on the wall was determined based on the results of a series of test calculations. At all χ values, the distance between the bubble center and the wall, which is slightly shorter than the longitudinal semi-axis of the bubble, was chosen so that the contact spot diameter always remained equal to 0.25 units of length. In this geometry, waves are focused near the wall center within a fairly wide region of gas of an increased density, thus enhancing the impact on the wall. The values of gas density in the bubble $\omega = 4.5$ and wave Mach number $M = 3.0$, which

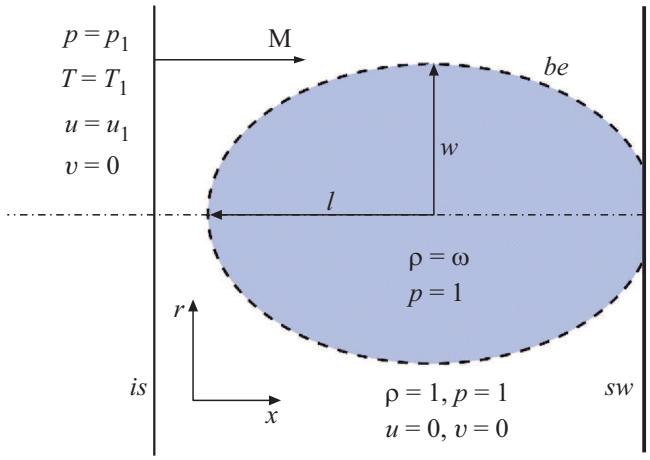

Figure 1. Diagram of the initial conditions. is is a shock wave propagating along axis x, be is the boundary of a bubble, sw is a solid wall, and l and w are semi-axes of an ellipsoid.

correspond to those providing the highest peak pressure on the wall in [7], were also taken as constants. The main adjustable parameter was the bubble shape, which varied within the range of $\chi = 0.5-1.5$ at a constant cross-section area.

Non-steady two-dimensional axially symmetric flows of ideal perfect gas were modelled based on Euler equations

$$\frac{\partial}{\partial t}\begin{pmatrix}\rho r\\ \rho u r\\ \rho v r\\ e r\end{pmatrix} + \frac{\partial}{\partial x}\begin{pmatrix}\rho u r\\ (p+\rho u^2) r\\ \rho u v r\\ (e+p) u r\end{pmatrix} + \frac{\partial}{\partial r}\begin{pmatrix}\rho v r\\ \rho u v r\\ (p+\rho v^2) r\\ (e+p) v r\end{pmatrix} = \begin{pmatrix}0\\ 0\\ p\\ 0\end{pmatrix},$$

where p, ρ, u, and v are the pressure, the density, and velocity components of gas along coordinate axes x and r, respectively, and $e = \frac{p}{\gamma-1} + \rho\frac{u^2+v^2}{2}$ is the total energy of a unit gas volume.

Numerical modeling was performed using the MacCormack method [8] augmented with Zhmakin–Fursenko conservative smoothing of non-physical oscillations [9] on a uniform square grid with 600 or 1200 points per unit length. A coarser grid was applied in calculations with varying χ, while a finer one was used to analyze the fine structure of focusing of shocks near the wall. The sufficiency of 600 grid points per unit length was established by analyzing the grid convergence of the numerical solution: all gas-dynamic flow elements were resolved completely on such a grid, and the values of integral measures of impulse impact on the wall were stabilized (see below). The computational domain was 1.3×1 units of length in size, ensuring that the boundaries were sufficiently spaced apart: possible weak perturbations propagating from the boundaries did not distort the examined flow region.

The shock flow pattern calculated for $\chi = 1.0$ is presented in Fig. 2. The gas density is represented by a color gradient, and solid black curves are pressure isolines (a color version of the figure is provided in the online version of the paper). The symmetry axis forms the lower boundary of figures; the white dashed curve denotes the initial bubble boundary. Shock wave ts transmitted into the bubble assumes a concave shape (due to the fact that its propagation velocity is lower than the one of initial wave is) and „overturns" with the formation of triple points tp and transverse shocks tss (Fig. 2, a). Shock rws is produced outside of the bubble as the external wave section undergoes reflection off the wall. Transverse shocks and triple points move along a diagonal to the symmetry plane and interact with section cws of the shock reflected off the wall that has penetrated into dense gas and propagates to the center of the wall (Fig. 2, b).

In the considered example, focusing shock cws reaches the symmetry axis earlier than shock ts reaches the wall. A different flow regime is established in the case of sufficiently oblate bubbles ($\chi < 0.85$): longitudinal shock ts propagates along the entire length of the bubble and gets reflected off the wall earlier than shock cws, which moves along the wall, reaches the symmetry axis. Subsequent focusing of transverse shocks proceeds in gas that was compressed in advance in the process of reflection of shock ts off the wall. At $\chi \approx 0.85$, longitudinal and transverse shocks reach the symmetry axis simultaneously.

Qualitative differences of the above flow regimes are revealed, for example, in „oscilloscope records" of pressure at the central point of the wall (Fig. 3, a). Dimensionless time $\tau = \frac{\mathrm{M}a_0}{2l}t$, where $2l$ is the longitudinal bubble diameter and $a_0 = \sqrt{\frac{\gamma p_0}{\rho_0}}$ is the speed of sound in the gas surrounding the bubble, is plotted on the horizontal axis of this diagram. The onset of interaction between an incident wave and the bubble boundary is assumed to correspond to $t = \tau = 0$; $\tau = 0.5$ is the moment when the unperturbed part of the incident wave reaches the center of the bubble, and $\tau \approx 1.0$ corresponds to the onset of reflection of the external wave off the wall. Horizontal lines in Fig. 3, a denote pressure $p = p_r = 51.67$ behind the reflected unperturbed wave (without the bubble) at $\mathrm{M} = 3.0$ and pressure $p = 117$ behind reflected wave ts (behind a plane wave in heavy gas).

In the case of oblate bubbles, the arrival of a plane wave, which has propagated along the entire length of the bubble, at the wall is characterized by a pressure increase to $p = 117$, and the subsequent pressure jump ($\tau = 1.66$ at $\chi = 0.7$) is induced by the arrival of shock cws at the symmetry axis. The pressure rise sequence for spherical bubbles ($\chi = 1.0$) is reversed: shock cws ($\tau = 1.43$) arrives first, followed by additional gas compression by the longitudinal wave ($\tau = 1.53$).

The peak pressure at the central point of the wall attained in the course of refraction and focusing of a shock wave has been adopted as the main measure of

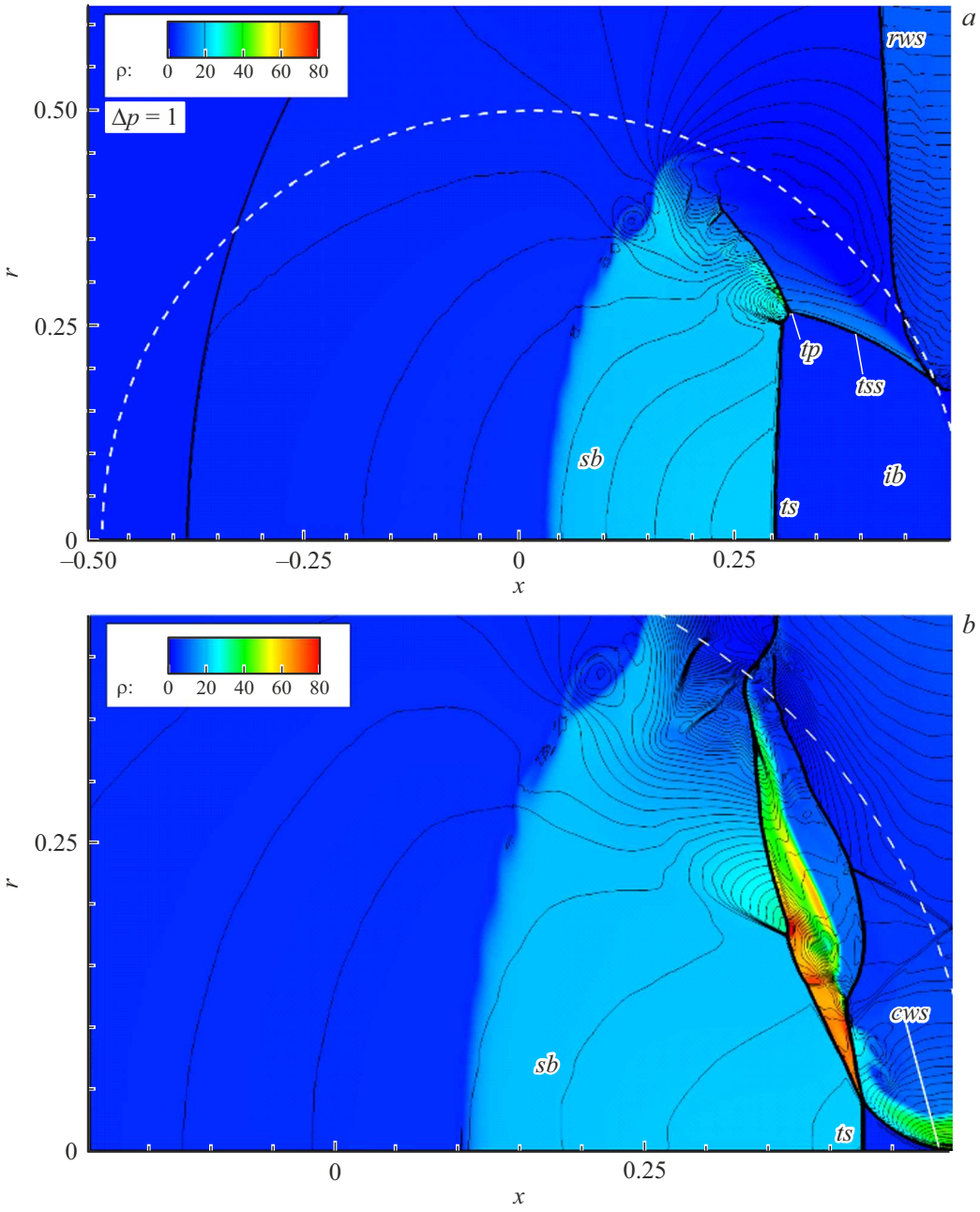

Figure 2. Key stages of flow at M = 3.0, $\omega = 4.5$, and $\chi = 1.0$: density field and pressure isolines with step $\Delta p = 1$ (a) and an exponential distribution (b). The lower boundary of the figure is the symmetry axis; the white dashed curve denotes the initial bubble boundary. The wall is at the right boundary of figures at $x = 0.5$. a — Formation of transverse shocks and reflection of an external shock off the wall; b — interaction of near-wall shocks with internal ones and focusing at the symmetry axis. ib and sb are unperturbed and shocked bubble regions, ts is a wave transmitted into the bubble, tp and tss are triple points and transverse shocks, rws is a shock reflected off the wall, and cws is a transverse shock converging to the symmetry axis.

shock impact on the wall in [7]. No grid convergence of the peak pressure is observed in an axially symmetric flow (see the table). This effect is related to a known phenomenon arising in the analysis of a cylindrical shock wave converging to a symmetry axis (Guderley problem): in an inviscid formulation, infinite pressure is attained at the moment of focusing. This effect manifests itself in numerical calculations as an unconstrained growth of the peak pressure (due to accompanying reduction of numerical viscosity) on finer grids.

In the present study, the following integral measures of the degree of impact on the wall were examined in addition to the peak pressure: (1) excess pressure impulse $I_p = \int_{t_0}^{t_f} (p - p_r)dt$ at the center of the wall, where t_0 corresponds to the onset of pressure rise at the center of

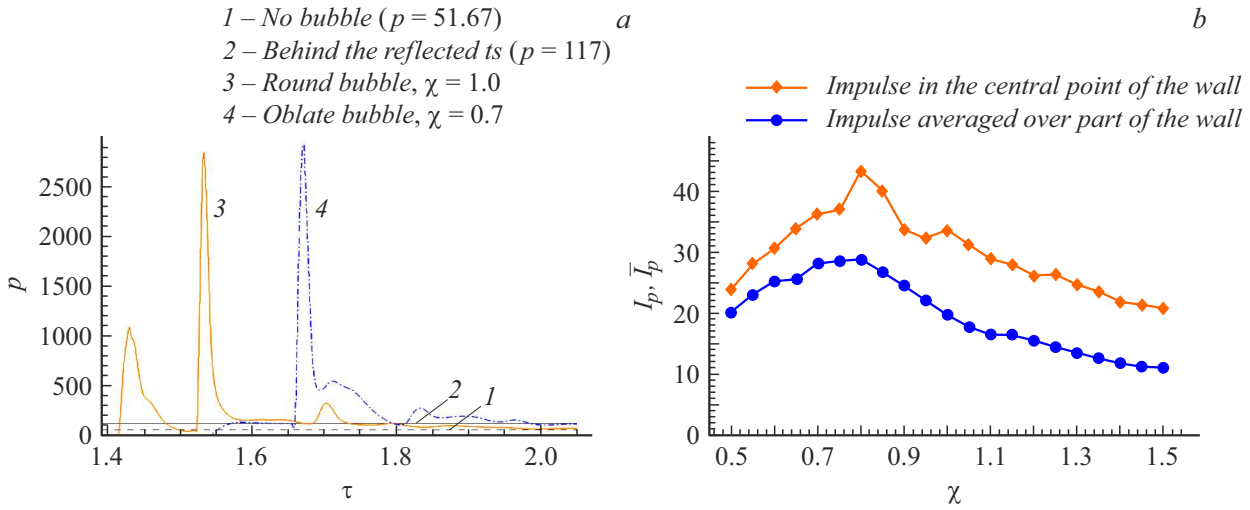

Figure 3. Typical dependence of the pressure at the central point of the wall on dimensionless time τ for two interaction modes (a) and dependences of single-point and averaged impulses of pressure on the wall on the bubble shape varying within the $0.5 \leqslant \chi \leqslant 1.5$ range (b). Straight lines $p = 51.67$ and 117 denote the pressure behind plane shock waves reflected off the wall (initial is and transmitted ts waves, respectively).

Dependence of peak pressure $p_{\max}$ at the center of the wall, excess pressure impulse I_p at the center of the wall, and impulse $\bar{I}_p$ averaged over a part of the wall on grid resolution in calculations for $\chi = 0.8$

Number of nodes points per unit length	$p_{\max}$	Impulse I_p	Averaged impulse $\bar{I}_p$
150	925	29.6	23.2
300	1784	35.6	27.1
600	2618	43.2	28.7
1200	3267	45.9	28.1

the wall and t_f is the final calculation time with $p \approx p_r$; (2) excess pressure impulse $\bar{I}_p = \frac{1}{S}\int\limits_S I_p ds$ averaged over section S of the wall with its diameter equal to one tenth of the radius of a spherical bubble. The convergence of a pressure impulse is vastly superior to that of the peak pressure, and an averaged pressure impulse gets stabilized already at 600 grid points per unit length (see the table). It is fair to assume that an averaged impulse is the most informative measure of shock impact on the wall, since its sensitivity to numerical viscosity is the lowest.

Figure 3, b presents the dependences of excess pressure pulses on the bubble shape varying within the range of $\chi =$ 0.5-1.5. Both pulses increase monotonically from $\chi = 0.5$ to the maximum at $\chi \approx 0.8$, wherein transverse shock cws is focused on the symmetry axis directly after the reflection of transmitted shock ts off the wall, and decrease as the bubble elongates further. The maximum of an averaged impulse exceeds the values for spherical and the most elongated bubbles by a factor of 1.5 and 2.5, respectively.

Two-dimensional numerical modeling was used to demonstrate that an ellipsoidal near-wall bubble of gas with an increased density provides a many-fold enhancement of an impulse impact on the wall induced by an incident shock wave. The greatest effect is achieved in the case of bubbles that are flattened slightly in the direction transverse to the shock wave motion and establish the conditions for fast consecutive compression of gas near the wall center in plane and cylindrical shocks.

Funding

This study was carried out at the Institute of Mechanics of the Moscow State University with the use of equipment provided by the Center for Collective Use of Ultra-High-Performance Computational Resources (Moscow State University) and with financial support from the Russian Science Foundation (project No. 21-11-00307).

Conflict of interest

The authors declare that they have no conflict of interest.

References

[1] D. Ranjan, J. Oakley, R. Bonazza, Ann. Rev. Fluid Mech., **43** (1), 117 (2011). DOI: 10.1146/annurev-fluid-122109-160744
[2] N. Haehn, D. Ranjan, C. Weber, J. Oakley, D. Rothamer, R. Bonazza, Combust. Flame, **159** (3), 1339 (2012). DOI: 10.1016/j.combustflame.2011.10.015
[3] P.Yu. Georgievskiy, V.A. Levin, O.G. Sutyrin, Shock Waves, **25** (4), 357 (2015). DOI: 10.1007/s00193-015-0557-4
[4] N. Haehn, C. Weber, J. Oakley, M. Anderson, D. Ranjan, R. Bonazza, Shock Waves, **22** (1), 47 (2012). DOI: 10.1007/s00193-011-0345-8

[5] B. Guan, H. Yang, H. Yang, G. Wang, Phys. Fluids, **34** (12), 126111 (2022). DOI: 10.1063/5.0130382
[6] Yu.V. Tunik, Fluid Dyn., **42**, 287 (2007). DOI: 10.1134/S0015462807020135.
[7] O.G. Sutyrin, R.R. Khabibullin, Fluid Dyn., **56**, 228 (2021). DOI: 10.1134/S0015462821020129.
[8] R.W. MacCormack, in *AIAA Hypervelocity Impact Conf.* (Cincinnati, Ohio, 1969), AIAA paper 69-354. DOI: 10.1142/9789812810793_0002
[9] A.I. Zhmakin, F.D. Popov, A.A. Fursenko, in *Algoritmy i matematicheskoe obespechenie dlya fizicheskikh zadach* (L., 1977), Vol. 2, pp. 65–72 (in Russian).

Translated by D.Safin